Society For Biomaterials

A novel coculture model of HUVECs and HUASMCs by hyaluronic acid micropattern on titanium surface

Jingan Li, Kun Zhang, Ying Xu, Jiang Chen, Ping Yang, Yuancong Zhao, Ansha Zhao, Nan Huang

Key Laboratory for Advanced Technologies of Materials, Ministry of Education, School of Material Science and Engineering, Southwest Jiaotong University, Chengdu 610031, People's Republic of China

Received 22 April 2013; revised 28 June 2013; accepted 1 July 2013
Published online 30 July 2013 in Wiley Online Library (wileyonlinelibrary.com). DOI: 10.1002/jbm.a.34867

Abstract: Orientation smooth muscle cell environment plays a positive role in the development of a functional, adherent endothelium. Therefore, building an orientation coculture model of endothelial cells (ECs) and smooth muscle cells (SMCs) on biomaterials surface may provide more help for understanding the interaction between the two cells *in vitro*. In the present study, a "SMCs-ColIV-ECs" coculture model was built on the hyaluronic acid (HA) patterned titanium (Ti) surface, and compared with the previous "SMCs-HAa-ECs" model on endothelial cell number, morphology index, nitric oxide (NO), and prostacyclin$_2$ (PGI_2) release, anticoagulation property, human umbilical artery smooth muscle cells (HUASMCs) inhibition property and retention under fluid flow shear stress. The result indicated that "SMCs-ColIV-ECs" model could enhance the number, spreading area, and major/minor index of human umbilical vein endothelial cells (HUVECs), which contributed to the retention of HUVECs on the surface. Greater major/minor index may produce more NO and PGI_2 release, contributing to the anticoagulation property and HUASMCs inhibition property. In summary, this novel "SMCs-ColIV-ECs" coculture model improved the previous "SMCs-HAa-ECs" model, and may provide more inspiration for the human vascular intima building on the biomaterials *in vitro*. © 2013 Wiley Periodicals, Inc. J Biomed Mater Res Part A: 102A: 1950–1960, 2014.

Key Words: coculture, endothelial cells, smooth muscle cells, micropattern, biomaterials

How to cite this article: Li J, Zhang K, Xu Y, Chen J, Yang P, Zhao Y, Zhao A, Huang N. 2014. A novel coculture model of HUVECs and HUASMCs by hyaluronic acid micropattern on titanium surface. J Biomed Mater Res Part A 2014:102A:1950–1960.

INTRODUCTION

Human vascular smooth muscle cells (SMCs), endothelial cells (ECs), and their interaction play an important role in maintenance of normal vascular structure and function.[1] Thus, the effect of ECs and SMCs interaction on vascular remodeling *in vivo* has attracted a lot of research.[2–4] However, this topic is extremely difficult because it is impossible to separate the effect of ECs or SMCs on SMCs and ECs interaction from all other factors within an artery *in vivo*.[5] Conventional cocultures present a reasonable way to model ECs and SMCs interaction *in vitro*[5–7]; however, they usually either fail to exhibit the endothelial regulatory effect on SMCs,[6,7] or fail to obtain a good anticoagulation property,[8] which is something expected to be seen from clinical observations.

In the previous work, we attributed these failures to the random distribution of the human umbilical vein endothelial cells (HUVECs) and human umbilical artery smooth muscle cells (HUASMCs), and therefore built an orientation coculture model of HUVECs and HUASMCs by hyaluronic acid (HA) microstrips on titanium (Ti) surface,[9] which metal has good biocompatibility and is the most widely used biomaterial for cardiovascular implants. The introduction of hyaluronidase (HAa) realized the transformation of HA from high molecular weiht (HMW) to the low molecular weight (LMW), thus improved the HUVECs adhesion on the low molecular weight hyaluronic acid (LMW-HA) microstrips,[9,10] and achieved the goal of orientation coculture of HUVECs and HUASMCs. Thus, the new coculture model was named "SMCs-HAa-ECs." Although the SMCs-HAa-ECs model was proved to release more nitric oxide (NO) as compared with the HUVECs cultured alone, the retention of HUVECs at third day was too low to ensure its function on vascular implant materials.

In the present study, we built a novel coculture model named "SMCs-type IV collagen (ColIV)-ECs," and found that the new coculture model obtained better ability of anticoagulation factors release, inhibiting HUASMCs proliferation and anticoagulation as compared with the SMCs-HAa-ECs model. It is noteworthy that the SMCs-ColIV-ECs model

Correspondence to: P. Yang; e-mail: yangping8@263.net
Contract grant sponsor: Key Basic Research Project; contract grant number: 2011CB606204
Contract grant sponsor: National Natural Science Foundation of China; contract grant numbers: 30870629, 50971107
Contract grant sponsor: Fundamental Research Funds for the Central Universities; contract grant numbers: SWJTU11ZT11; SWJTU11CX054
Contract grant sponsor: Open Research Fund of State Key Laboratory of Bioelectronics, Southeast University

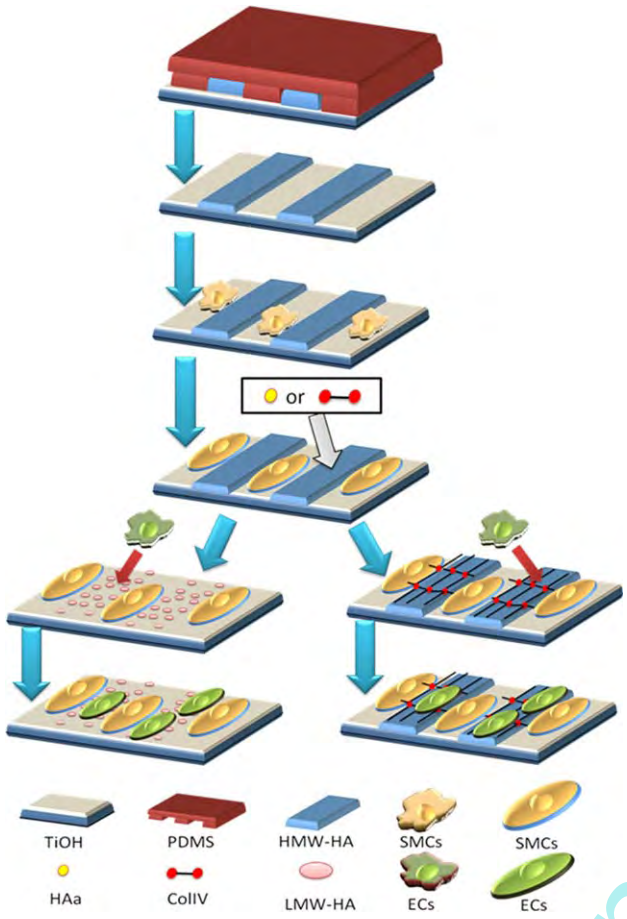

FIGURE 1. The scheme of coculturing endothelial cells and smooth muscle cells on TiOH substrate. [Color figure can be viewed in the online issue, which is available at wileyonlinelibrary.com.]

could significantly enhance the retention of HUVECs on the biomaterials surface. These data may be helpful to bionicly building the coculture model of HUVECs and HUASMCs *in vitro*, and provide potential theoretical basis for the treatment of cardiovascular disease.

EXPERIMENTAL

Preparation of hyaluronic acid micropattern on titanium surface

The parallel microstrips of high molecular weight hyaluronic acid (HMW-HA) were prepared to mirror-polished and then alkali activated Ti (Baoji, China) surface using a soft lithography method. The detailed description of the process can be read in our previous work.[9] In this study, the micropatterned substrate was used to build a novel coculture model of HUVECs and HUASMCs when compared with the previous one[9] (Fig. 1).

Morphology characterization of the substrates (AFM and OM)

The surface topography was depicted using a Nanowizard II AFM (JPK Instruments, Berlin, Germany) in tapping mode. AFM was performed at 25°C in air at a rate of one line scan per second. Images were analyzed using the CSPM Imager software. The distance between every two HA microstrips was marked in an optical microscopy (OM) photograph, which was obtained under a phase contrast microscope (DMRX, Leica, Germany).

XPS analysis

The elemental chemical surface composition was detected by XPS on an AXIS HSi spectrometer (Kratos Analytical Ltd, UK) using an AlKa X-ray source (1486.6 eV photons, 150 W). The pressure in the chamber was below 2×10^{-9} Torr, and the binding energy scale was referenced by setting Cls peak at 284.6 eV.[11]

Water contact angle measurement

Sessile water contact angles (WCA) on substrates surface were measured on a contact angle instrument (JY-82, China) at room temperature. A minimum of three values of contact angles were collected per each group of samples.

HUVECs culture

HUVECs were isolated and cultured using the method according to the previous work.[9,12] In brief, human umbilical vein was clamped after filling with M199 medium (Hyclone Company) containing 0.1% collagenase II (Invitrogen Corporation). After incubation for 12 min at 37°C, digestion was quenched by adding M199 medium with 20% fetal bovine serum (FBS, Hyclone Company). HUVECs were collected after centrifugation of the digested cell suspension. Harvested cells were resuspended in M199 medium with 20% FBS, then added into a culture flask and incubated in a humidified incubator with 5% CO_2 at 37°C. Subculture was performed when the confluency was obtained, and cells were used at third passage.

HUASMCs culture

Primary culture of HUASMCs were performed by slow outgrowth from small pieces of umbilical artery media layer under standard cell culture conditions in DMEM/ F12 medium with 10% FBS.[9] The culture medium was changed every 2 days. Subculture was performed when the confluency was obtained, and the third cells were used for the experiment.

HUASMCs attachment

HUASMCs were seeded on the surfaces of the TiOH and TiOH/HAP samples at the concentration of 1×10^5 cells/mL after stained by the cell tracker in orange color (CMTMR, Invitrogen), and then cultured in a humidified incubator with 5% CO_2 at 37°C for 4 h, finally observed under an inverted optical microscope (OLIMPUS-IX51, Japan). Cell proliferation was examined using a CCK-8 assay.[13] The SMCs used for CCK-8 (BD Biosciences, San Jose, CA) detection was nonstained.

Co-culture of HUVECs and HUASMCs

Two coculture models of HUVECs and HUASMCs were built to enhance the anticoagulation and inhibitory hyperplasia

properties of the HUVECs, the HUVECs cultured alone on the TiOH surface were used as control. Briefly, HUASMCs marked in orange color were seeded on the patterned samples as description in section "HUASMCs attachment". The following step were the differences between the two models: in Model 1, 30 μL hyaluronidase (HAa, Sigma-Alrich) was dropped on to the patterned HUASMCs and incubated at 37°C for 2 h, rinsed with warm PBS; in Model 2, 30 μL of 500 μg/mL Collagen IV (ColIV, Sigma-Alrich, diluted in acetate buffer, pH = 4.5) was introduced to the surface and incubated at 37°C for 20 min. The final steps were same for both model, HUVECs marked with green tracker (CMFDA, Invitrogen) were seeded on the samples at the concentration of 1×10^5 cells/mL and incubated at 37°C for 1 day and 3 days. After a rinsed operation, the cells fixed with 2.5% glutaraldehyde for 2 h were observed by fluorescence microscope. HUVECs number and morphology index including spreading area, orientation angle, and major/minor index from 15 random optical microscope fields were counted and calculated statistically by Image J Launcher (Broken Symmetry Software).[14]

NO and PGI_2 release of HUVECs

The amount of NO and PGI_2 released from HUVECs on each sample were detected to evaluate the anticoagulation and inhibitory hyperplasia properties of the HUVECs preliminarily. The NO release was examined by a typical Griess Reagent method as described in the previous work,[9] and the PGI_2 detection was performed by ELISA kit according to the manual after 1 and 3 days incubation. The amount of NO and PGI_2 were finally normalized to cell number.

Calculation of fluorescence intensity ratio of HUVECs and HUASMCs

For further investigating and comparing the inhibitory hyperplasia property of the HUVECs of the two models, the fluorescence intensity ratios of the HUVECs (green) and *HUASMC*s (orange) in different coculture models were measured and calculated by Ipwin32 Application (Media Cybernetics). The larger ratio was defined as the better inhibitory hyperplasia property of the HUVECs in coculture models. A 3D fluorescence intensity images were generated to display the direct and visual effect of the statistical data.

Function of anticoagulation

Platelet adhesion and activation. In brief, human platelets rich plasma (PRP) obtained from fresh whole blood of a volunteer was thawed at 37°C, and 30 μL of the PRP was added to TiOH samples which had been immersed in the used medium (FBS free) collected from SMCs-ColIV-ECs, SMCs-HAa-ECs, and HUVECs group (1 day) for 2 h, and incubated at 37°C for 15 min. After rinsed with PBS for three times, the adherent platelets were fixed with 4% paraformaldehyde for 0.5 h at room temperature. The fluorescence images of adherent platelets were obtained after Rhodamine reagent staining. Platelet adhesion and activation were determined using the method of LDH and GMP140, respectively.[15]

Clotting time of the whole blood. Clotting time of the mixtures composed of the whole blood and the used medium in ratio of 1:1 were statistically measured.

Retention of HUVECs

Retentions of HUVECs in SMCs-ColIV-ECs, SMCs-HAa-ECs, and HUVECs groups were detected using the previous method.[9]

Data analysis

The data was analyzed by the software SPSS 11.5 (Chicago, IL). The data were expressed as mean ± standard deviation (SD). The probability value $p < 0.05$ was considered significant.

RESULTS AND DISCUSSION

Preparation of the HMW-HA microstrips on the Ti surface

The preparation process of the HMW-HA micropattern to the alkali activated Ti substrate was depicted and confirmed by AFM, OM, XPS, and WCA. AFM was performed to see the surface roughness change during the fabricated process. As shown in Figure 2(A), the surface roughness of Ti substrate [Fig. 2(A-a), 8.6 ± 0.7 nm] increased through the hot NaOH solution treatment [Fig. 2(A-b), 17.1 ± 1.4 nm], and then decreased to a much lower value [Fig. 2(A-c), 0.6 ± 0.2 nm] by introducing the HA coating. After the HA coating patterned by soft lithography method, the surface roughness achieved the top value in the whole fabrication [Fig. 2(A-d), 27.4 ± 47.1 nm]. The boundary of the HA strip and TiOH strip could be clearly seen on the image [Fig. 2(A-d)], and the drop gap may be the reason why the roughness on the TiOH/HA surface increased. As Li et al. described,[16] the surfaces should be smoother and the roughness at the level of protein adsorption for implants in contact with blood such as artificial heart valve and cardiovascular stents (<50 nm), otherwise may lead to platelet adhesion, activation, and further thrombogenesis. Our results demonstrated that the roughness of TiOH/HAP was small enough even used for blood contact devices, and the large roughness of TiOH surface contributed to the physical adsorption of the HA.

OM image was obtained to show the overview of the TiOH/HAP and the breadth of the TiOH strip and HA strip. In our study, the breadth of the strips was still both 25 μm [Fig. 2(B)], consistent with the previous parameter.[9] The microgrooves for HUASMCs could be 15–70 μm but only the micrometers ranged from 20 to 30 μm for HUVECs instead.[17] The OM images might be the evidence for confirming integrity of the micropattern so called cell template.

XPS analysis was carried out to analyze chemical compositions of each substrate. The XPS widescan spectra of the samples and their corresponding surface elemental compositions are shown in Figure 3. Carbon was typically derived from unavoidable hydrocarbon contamination, and it was used as an internal reference at 284.6 eV for calibrating peak positions. When compared with Ti surface, new Ca2p peaks (346.9 eV) appeared in the spectrum of TiOH and TiOH/HA and TiOH/HAP samples, and this may be

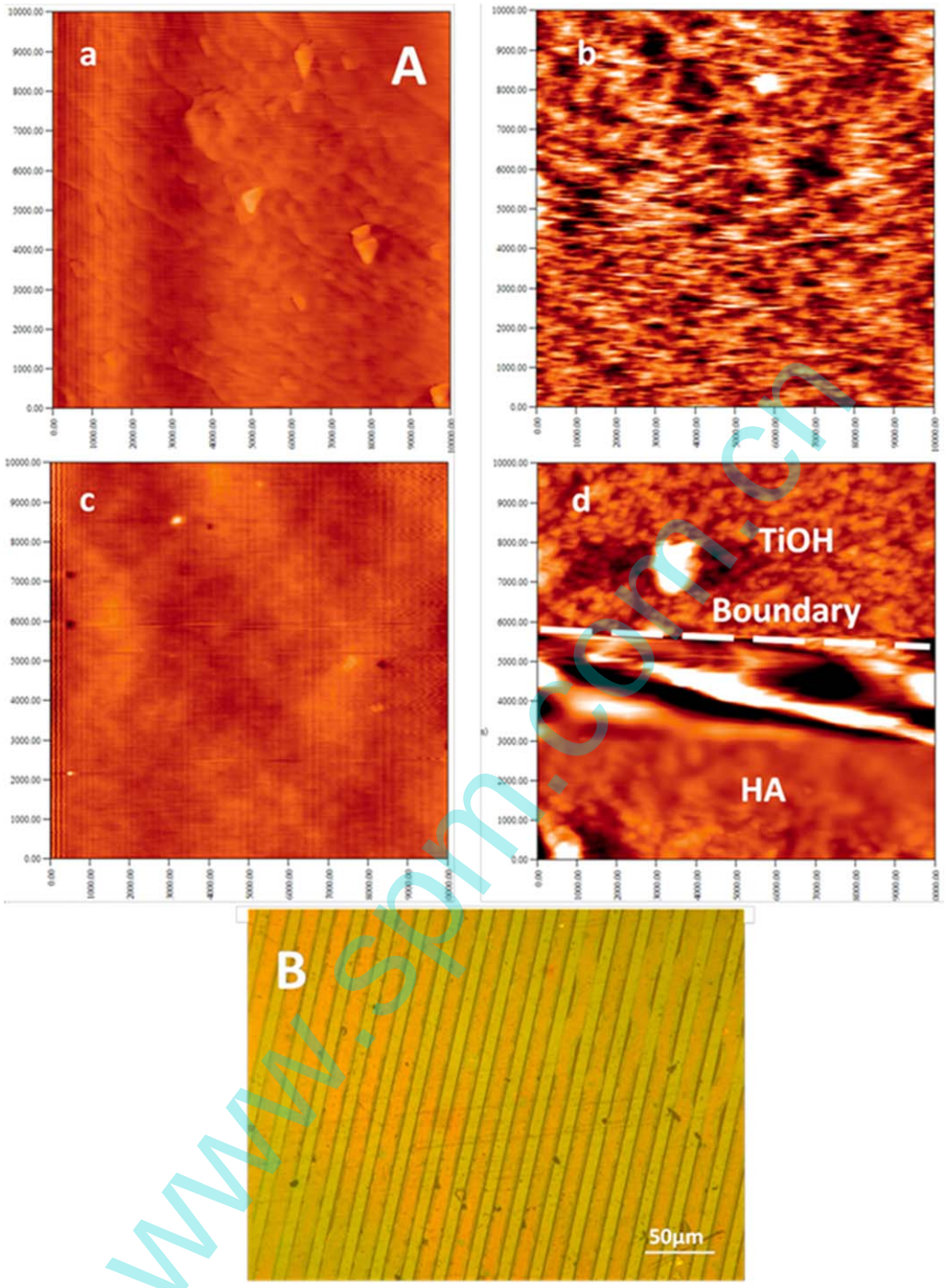

FIGURE 2. (A) The AFM images of (a) Ti, (b) TiOH, (c) TiOH/HA, and (d) TiOH/HAP; (B) Optical microscopy image of TiOH/HAP. [Color figure can be viewed in the online issue, which is available at wileyonlinelibrary.com.]

attributed to the calcium contamination of NaOH during their preparation. Ti2p peaks (460 eV) decreased and new N1s peaks (400 eV) appeared corresponding to TiOH/HA and TiOH/HAP samples, indicating the successful grafting of HA. The XPS results indicated that the HA micropattern had been prepared on to the TiOH surface in chemical aspect.

WCA measurement was performed as a function of process of Ti substrate (Fig. 4). Compared with Ti, the WCA dramatically decreased to about $10.3 \pm 0.9^\circ$ after activation by NaOH, while increased to $29.8 \pm 3.6^\circ$ after introducing HA, indicating that the TiOH/HA surfaces were more hydrophobic than TiOH surfaces. After the pattern-press process, the value decreased to $23.6 \pm 1.2^\circ$ due to the exposure of the TiOH strips. The WCA changes indicated the surface wettability change of each process step, also indirectly confirmed the successful preparation of the HA micropattern on the Ti substrate.

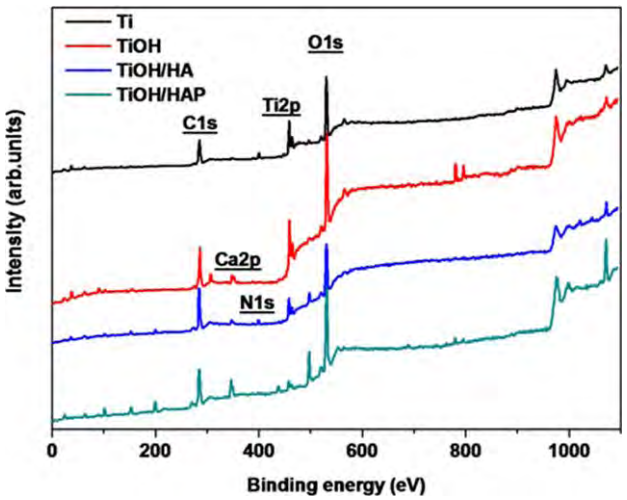

FIGURE 3. XPS spectra of Ti, TiOH, TiOH/HA, and TiOH/HAP. [Color figure can be viewed in the online issue, which is available at wileyonlinelibrary.com.]

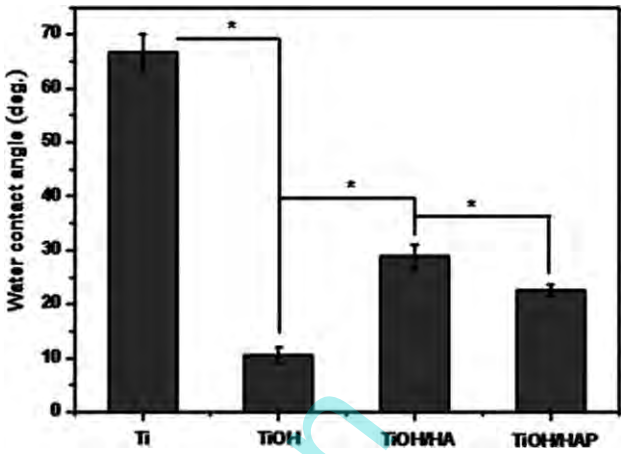

FIGURE 4. The water contact angle of each sample ($N = 5$, mean ± SD, $^*p < 0.05$).

Effect of HMW-HA microstrips on HUASMCs regulation

Figure 5(A) shows the morphology of HUASMCs on the TiOH/HAP and TiOH surfaces after cultured for 4 h. It could be seen that the HUASMCs (red) on the TiOH surface exhibited multilateral or amorphous morphology and possessed more spreading area, while the HUASMCs seeded on the TiOH/HAP surface showed long spindle-shaped morphology. Compared the random orientation of HUASMCs on the TiOH surface, the HUASMCs on the TiOH/HAP surface grew along with the microstrips in a parallel orientation. The absorbance of CCK-8 values, which is positively correlated to the cell number, was also different on each surface [Fig. 5(B)]. The absorbance on the TiOH/HAP surface was significantly smaller than that on the TiOH surface ($p < 0.05$). All these results indicated that the HUASMCs spreading were inhibited by HMW-HA and the adhesion, proliferation, and migration behavior of HUASMCs on the TiOH/HAP surface was controlled by the HMW-HA microstrips.

Coculture of HUASMCs and HUVECs in two models

Figure 6(A) shows the HUVECs amount on each sample after culture of 1 day and 3 days, respectively. The TiOH sample remained the remarkable advantage of HUVECs amount as compared with the both coculture samples. There was no significant difference between the two coculture models on HUVECs amount after culture of 1 day. However, the SMCs-ColIV-ECs model exhibited a significantly larger HUVECs amount than the SMCs-HAa-ECs model, indicating that the new model may be an effect approach to enhance the HUVECs coverage as well as their anticoagulant function.

As shown in Figure 6(B), the HUASMCs (red) on all samples in the coculture exhibited long spindle-shaped morphology and formed several long stripes, and HUVECs (green) grew between two adjacent HUASMCs stripes and exhibited polarized form along the stripes direction. Its interesting that the elongated HUVECs of SMCs-ColIV-ECs still distributed in the HUASMCs-blank area but not on the HUASMCs as expected previously. After culturing for 3 days, the HUVECs of SMCs-ColIV-ECs model could not limit or cover the HUASMCs either. Only few HUVECs attached on the surface of the HUASMCs, but not showing a spreading or elongated morphology. Compared with HUASMCs cultured for 1 day, the muscle cells cultured of 3 days exhibited remarkably increased spreading area visually. This result was consistent with the HUVECs behavior on HUASMCs described by Tu et al.[17] Their study demonstrated that a low-density of HUASMCs and a high-density of

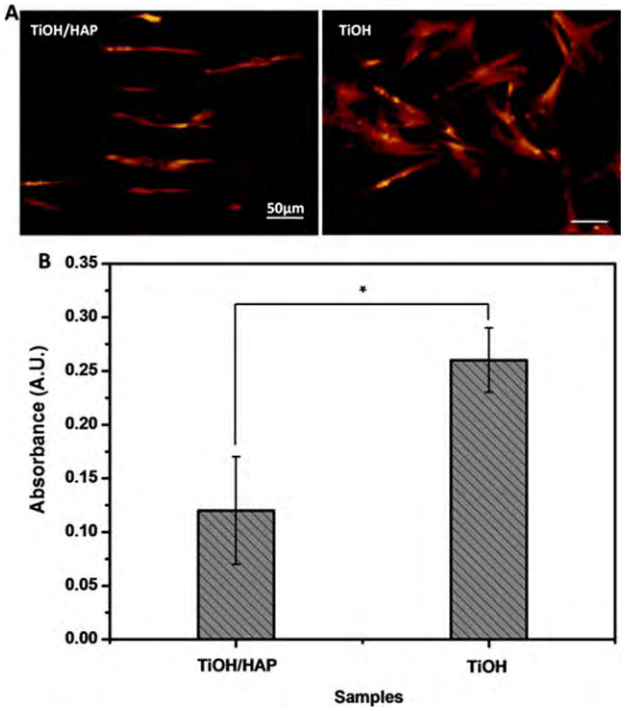

FIGURE 5. (A) Fluorescence graphic of SMCs on TiOH and TiOH/HAP; (B) Detection of adherent SMCs on TiOH and TiOH/HAP using a CCK-8 aassay ($N = 5$, mean ± SD, $^*p < 0.05$). [Color figure can be viewed in the online issue, which is available at wileyonlinelibrary.com.]

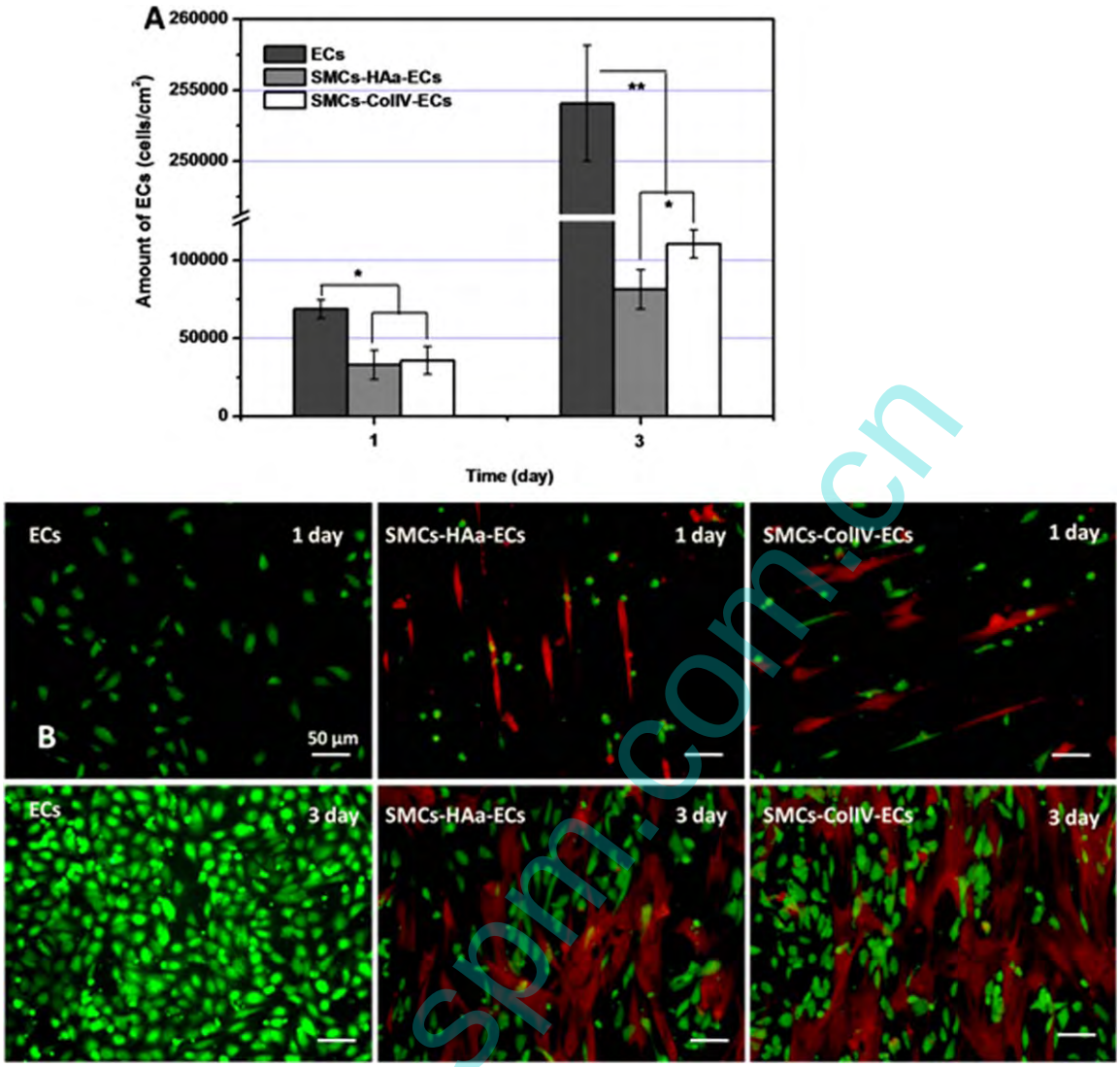

FIGURE 6. (A) Amount of ECs in the groups of ECs alone, SMCs-HAa-ECs and SMCs-ColIV-ECs, respectively ($N = 5$, mean ± SD, $*p < 0.05$, $**p < 0.01$); (B) Fluorescence graphics of SMCs (red) and ECs (green) in the groups of ECs alone, SMCs-HAa-ECs and SMCs-ColIV-ECs, respectively. [Color figure can be viewed in the online issue, which is available at wileyonlinelibrary.com.]

HUVECs was necessary for the coculture of the two cells, and this experimental will be performed in our next work, while this study will focus on the anticoagulant and inhibiting HUASMCs proliferation function of the new model as compared with the SMCs-HAa-ECs.

Calculation of HUVECs morphology index

Figure 7 displays the morphology index of the HUVECs including spreading area, orientation angle, and major/minor index. It could be seen that the spreading area of the HUVECs of SMCs-ColIV-ECs model increased compared with the SMCs-HAa-ECs model and showed no significant difference compared with the HUVECs cultured alone [Fig. 7(A)]. This may be attributed to the introduction of the CoIV, which can improve cell spreading on the surface.

The orientation angle represents the cell orientation degree, which is controlled by the surface physical topology or chemical composition. The HUVECs cultured alone on TiOH for 1 and 3 days were in an extremely random state, presenting the large orientation angle of $40.58 \pm 18.33^\circ$ and $51.36 \pm 19.69^\circ$, respectively [Fig. 7(B)]. The orientation angle of HUVECs of SMCs-HAa-ECs model and SMCs-ColIV-ECs model were $10.96 \pm 3.37^\circ$ and $5.14 \pm 1.29^\circ$, respectively at first day, and $12.78 \pm 1.35^\circ$ and $9.66 \pm 4.73^\circ$, respectively at third day, indicating that the HUVECs were aligned along with the HUASMCs microstrips. It demonstrated that the orientation of the HUVECs could also be strictly controlled by the HUASMCs micropattern in the new coculture model.

The major/minor index represents the cell elongation degree on the surface. It has been reported that the elongated HUVECs released more NO and PGI_2 which contribute to anticoagulation and inhibiting the excessive proliferation of the HUASMCs. As shown in Figure 7(C), HUVECs of the SMCs-ColIV-ECs model exhibited a significant larger major/

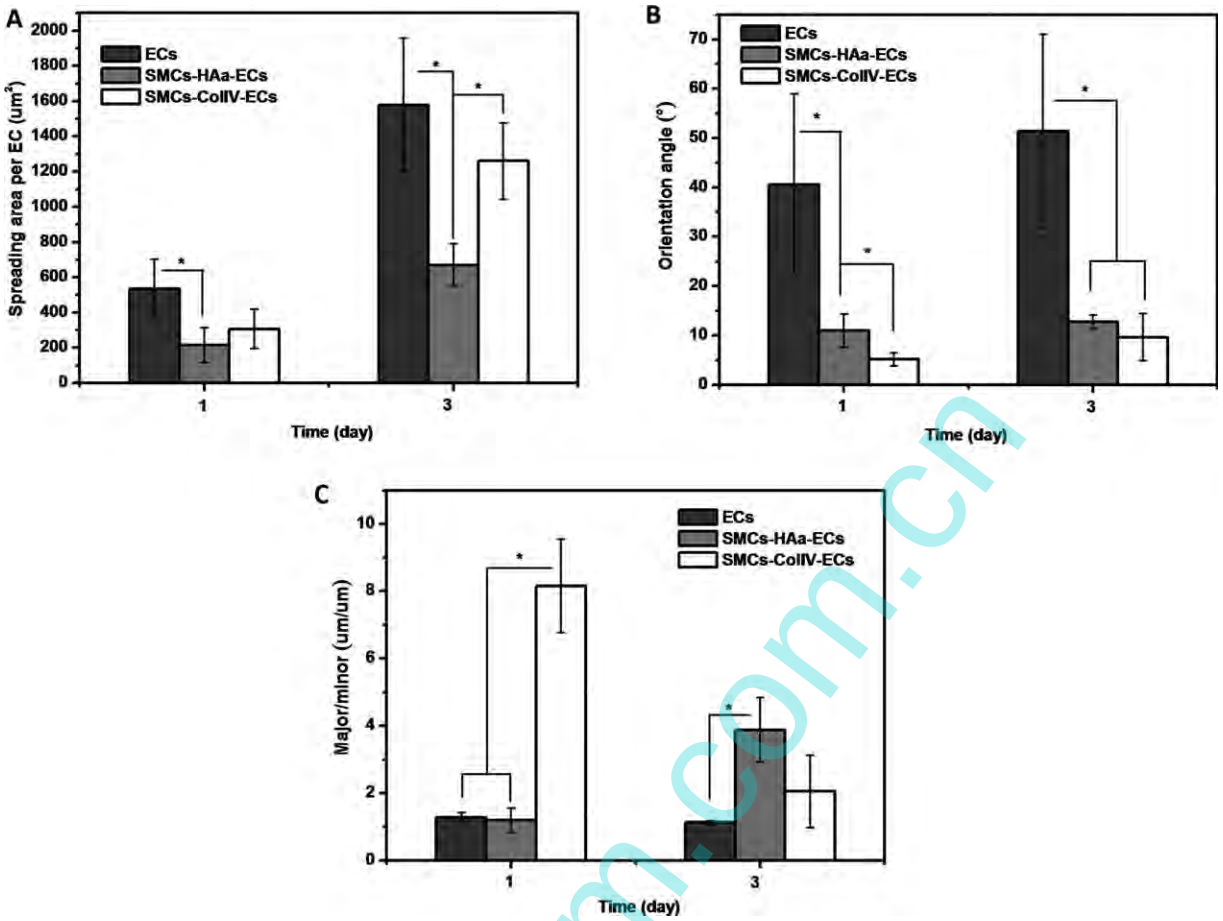

FIGURE 7. The calculation of the morphology index of ECs: (A) spreading area; (B) orientation angle; (C) Major/minor ($N = 5$, mean $\pm$ SD, $^*p < 0.05$).

minor index as compared with HUVECs of SMCs-HAa-ECs model and HUVECs cultured alone at first day, while HUVECs of SMCs-HAa-ECs model possessed the advantage as compared the other groups at third day. The reduction of the major/minor index in SMCs-ColIV-ECs model may be the interaction between ColIV and HA,[18] which could reduce the HA micropattern ability on limiting the cells.

NO and PGI_2 release

Nitric oxide (NO) plays an important role in controlling several physiological functions of the cardiovascular system.[19] NO can react with $O_2^{+,-}$, forming the powerful oxidant peroxynitrite ($ONOO^-$), which seems to take part in protein oxidation reactions under physiological conditions.[20,21] NO or nitrosonium can form *S*-nitrosothiols by reacting with sulfhydryl groups, which are potent platelet aggregation inhibitors and vasorelaxant compounds contributing to inhibiting HUASMCs proliferation.[20,22]

The results of NO release detection are displayed in Figure 8(A). NO released by HUVECs in SMCs-ColIV-ECs model was 90.1 ± 1.1 nmol/10^3 cells compared with the amount of 36.5 ± 2.4 nmol/10^3 cells released by HUVECs in SMCs-HAa-ECs model and 6.9 ± 1.3 nmol/10^3 cells released by HUVECs alone at first day, and NO released by HUVECs in SMCs-ColIV-ECs model was 70.4 ± 5.9 nmol/10^3 cells compared with the amount of 66.0 ± 12.5 nmol/10^3 cells released by HUVECs in SMCs-HAa-ECs model and 5.1 ± 2.2 nmol/10^3 cells released by HUVECs alone at third day. It is obvious that SMCs-CoIV-ECs model released more NO than SMCs-HAa-ECs model at first day while there was no significant difference between the two models at third day. Both coculture models released more NO than HUVECs alone at first day and third day. This result was consistent with the major/minor index in section "Calculation of HUVECs morphology index" suggesting that the elongation of HUVECs by microstrips or mechanical stimulation of HUASMCs contribute to more NO release, and this stimulation may be similar to the fluid flow shear stress (FFSS).[23]

In 1976, a novel eicosanoid extracted from the aortas of sheep and pigs was firstly found and initially termed PGX by the research team, while further research found that a synthetic form of this molecule was over 30 times more potent than PGE_2 in inhibiting human platelet aggregation, and the molecule was also found to cause relaxation of smooth muscle constriction of gastrointestinal muscles, and was later renamed PGI_2.[24,25]

Figure 8(B) shows the results of PGI_2 release by HUVECs in SMCs-ColIV-ECs, SMCs-HAa-ECs, and HUVECs groups,

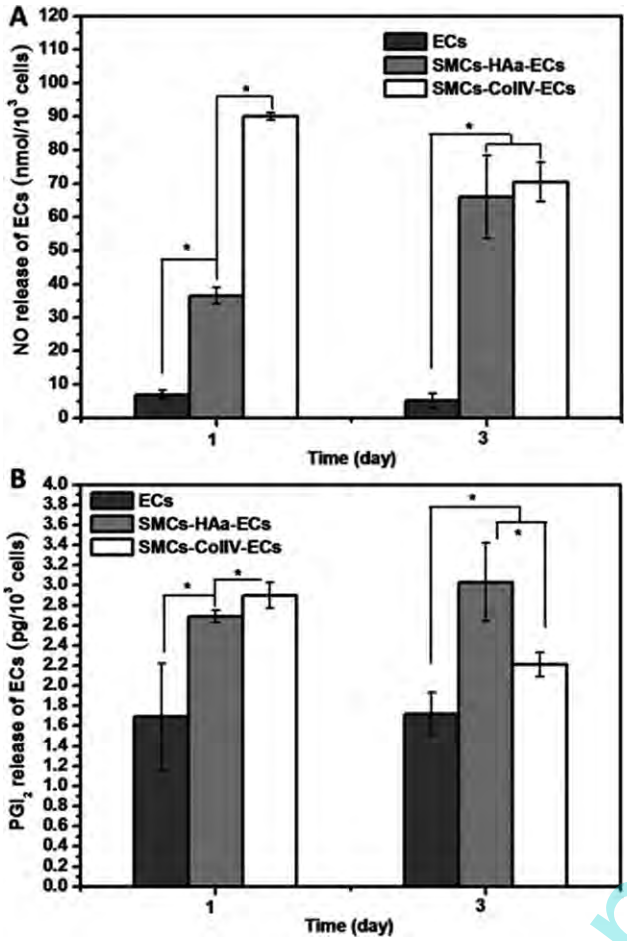

FIGURE 8. (A) The amount of NO released from each group; (B) the amount of PGI2 released from each group ($N = 10$, mean ± SD, $^*p < 0.05$).

respectively. PGI_2 released by HUVECs in SMCs-ColIV-ECs model was 2.9 ± 0.1 pg/10^3 cells compared with the amount of 2.7 ± 0.1 pg/10^3 cells released by HUVECs in SMCs-HAa-ECs model and 1.7 ± 0.5 pg/10^3 cells released by HUVECs alone at first day, and PGI_2 released by HUVECs in SMCs-ColIV-ECs model was 2.2 ± 0.1 pg/10^3 cells compared with the amount of 3.0 ± 0.4 pg/10^3 cells released by HUVECs in SMCs-HAa-ECs model and 1.7 ± 0.2 pg/10^3 cells released by HUVECs alone at third day. Obviously, SMCs-ColIV-ECs model released more PGI_2 than SMCs-HAa-ECs model at first day but less amount than the latter at third day. Both coculture models released more PGI_2 than HUVECs alone at first day and third day. This result was also consistent with the major/minor index and NO release, and it indicated that the elongation of HUVECs by mechanical effect contribute to more PGI_2 release because PGI_2 is formed from cell membrane phospholipids that enter the arachidonic acid metabolic pathway.[24,26]

Function of inhibiting proliferation of HUASMCs

Calculation of fluorescence intensity ratio of HUVECs (green) and HUASMCs (red) in the two models was performed to investigate the HUVECs function on inhibiting proliferation of HUASMCs (Fig. 9). The ratio of SMCs-ColIV-ECs model was 1:2.28 compared with 1:3.15 of SMCs-HAa-ECs model at first day, and the ratio of SMCs-ColIV-ECs model was 1:0.81 compared with 1:0.92 of SMCs-HAa-ECs model at third day. The ratio of HUVECs group was defined as 1:0 because no HUASMCs existed here. Obviously, the SMCs-ColIV-ECs model possessed larger ratio than the SMCs-HAa-ECs model at first day and third day, respectively. The reason may be that the ColIV layer covered on the HUASMCs limit the proliferation of the HUASMCs and the NO and PGI_2 released by the HUVECs also play important

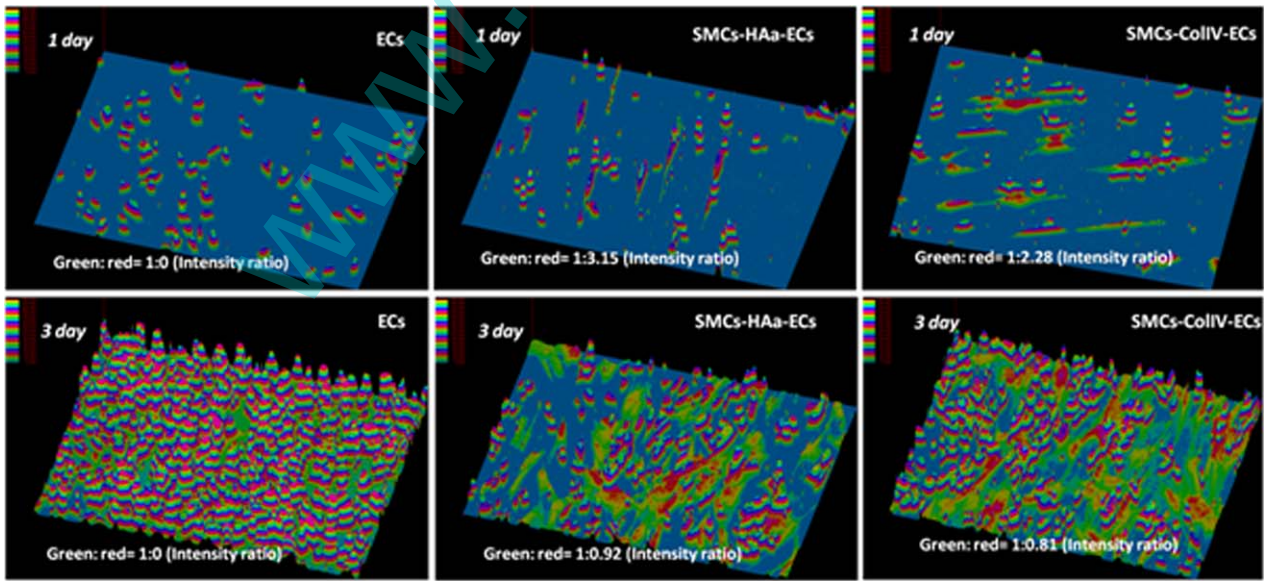

FIGURE 9. Three-dimensional fluorescence imaging graphics and the fluorescence intensity ratios of ECs and SMCs in each group. [Color figure can be viewed in the online issue, which is available at wileyonlinelibrary.com.]

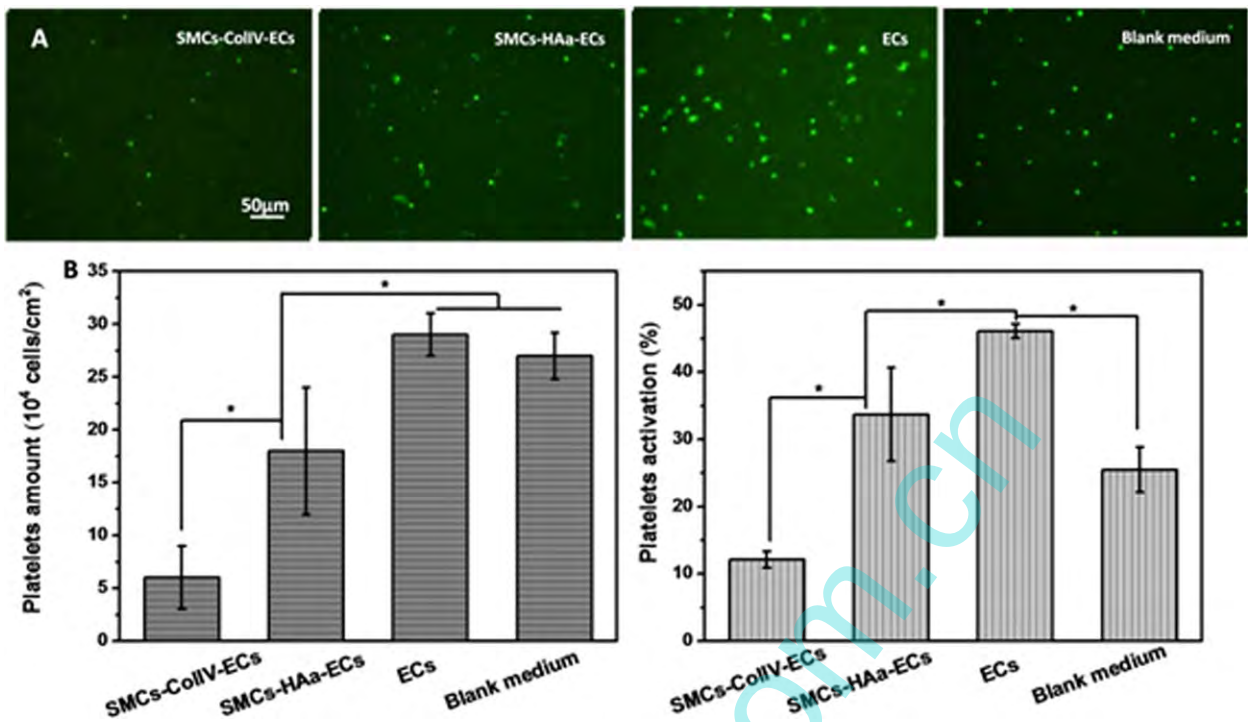

FIGURE 10. (A) Fluorescence image of adherent platelets on TiOH immersed in FBS-free medium of (a) SMCs-ColIV-ECs, (b) SMCs-HAa-ECs, (c) ECs, and (d) blank medium; (B) The number of adherent and activated platelets on TiOH immersed in FBS-free medium of each group ($N = 3$, mean ± SD, $*p < 0.05$ as compared with the other groups). [Color figure can be viewed in the online issue, which is available at wileyonlinelibrary.com.]

role. The NO and PGI_2 release of SMCs-HAa-ECs model at third day and compared with the value at first day as shown in Figure 8 may contribute to the effectively inhibiting on HUASMCs proliferation. This calculation result indicated that the SMCs-ColIV-ECs model possess better ability on inhibiting HUASMCs proliferation compared with the SMCs-HAa-ECs model. However, this is just a statistical result, more evaluation and detection should be done to confirm it in the future work.

Function of anticoagulation

Platelet adhesion. Figure 10 A depicts the fluorescence image of the adherent platelets on TiOH, which had been immersed in used medium of SMCs-ColIV-ECs, SMCs-HAa-ECs, HUVECs alone, and the blank medium, respectively. The platelets on SMCs-ColIV-ECs group TiOH, SMCs-HAa-ECs, and the reference group TiOH showed spherical morphology compared with spreading, polygonal, and pseudopodia extending morphology on HUVECs alone groups TiOH. The statistical result in Figure 10(B) also showed that the amount and activation of adherent platelets on SMCs-ColIV-ECs group TiOH was significantly less than the data of SMCs-HAa-ECs, HUVECs alone and the reference groups TiOH. All the results indicated that the SMCs-ColIV-ECs coculture model own better antiplatelet-adhesion ability than SMCs-HAa-ECs and HUVECs alone.

Clotting time of the whole blood. The clotting time of the mixture composed of the whole blood and used medium (FBS free) collected from each group in ratio of 1/1 after incubation of 1 day was applied in the evaluation of *in vitro* antithrombogenicity of the HUVECs, and the results are shown in Figure 11. The SMCs-CoIV-ECs group and SMCs-HAa-ECs group showed a significantly prolonged clotting time when compared with the HUVECs group and the control groups suggesting that the morphology elongation and

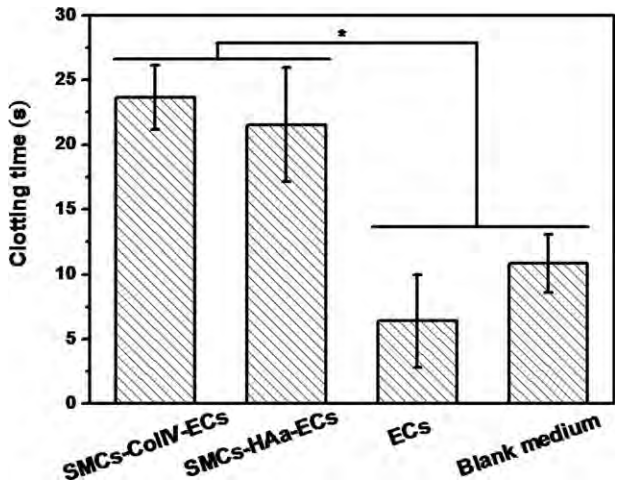

FIGURE 11. Clotting time of the mixtures of the whole blood and used medium (FBS free) collected from each group in ratio of 1:1 after incubation of 1 day ($N = 3$, mean ± SD, $*p < 0.05$ compared with the other groups). The blank medium was used as control.

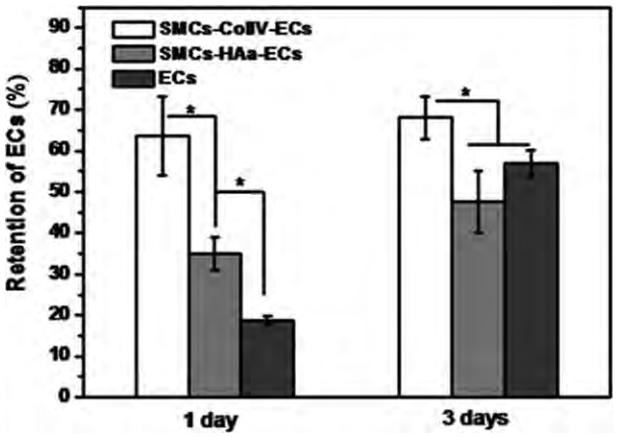

FIGURE 12. Retention of ECs in SMCs-ColIV-ECs and SMCs-ColIV-ECs co-culture model. EC cultured alone on TiOH samples were used as control (mean ± SD, $*p < 0.05$).

the present of the HUASMCs could enhance the anticoagulation function of the HUVECs.

The vascular intima injury and the exposure of HUASMCs below have been considered as the main reason of the atherosclerosis for a long time. In fact, it has been proved that the ECM of the HUASMCs also own good blood compatibility,[27] and our work also obtain the same results. The reason may be more release of the anticoagulant, such as NO and PGI_2. There is perhaps some unknown physiological responses in this process. More work will be done to discover the further mechanism.

Retention of HUVECs

The reduced retention of HUVECs in SMCs-HAa-ECs group at third day compared with HUVECs alone was the problem, which had not been solved in the previous work.[9] We attributed this result to the barrier of micropatterned HUASMCs. In the present study, we built a vertically distributed coculture model by introducing the ColIV layer to solve this problem. Figure 12 displayed the retention of ECs in SMCs-ColIV-ECs, SMCs-HAa-ECs, and HUVECs alone models. Undoubtedly, SMCs-ColIV-ECs showed a significantly higher retention of HUVECs as compared with the SMCs-HAa-ECs and HUVECs alone models, which indicated that the SMCs-ColIV-ECs offered a better protection for HUVECs from the FFSS scouring. This may be due to the fiber network structure of the ColIV, which contributed to the adhesion and spreading of the HUVECs.

CONCLUSIONS

In this study, two coculture models of HUVECs and HUASMCs were built on the HA microstrips on titanium surfaces, respectively. The HUASMCs in the two coculture models were both effectively modulated by the HA microstrips, and the HUVECs were effectively modulated by the HUASMCs microstrips, while HUVECs of SMCs-ColIV-ECs got better spreading areas as compared with those of SMCs-HAa-ECs. On the aspect of secretion, HUVECs of SMCs-ColIV-ECs release more NO and PGI_2 compared with HUVECs of SMCs-HAa-ECs and HUVECs alone at the first day, thus obtaining better coagulation property in the platelet adhesion, activation, and whole blood clotting time test. A quantitative method of fluorescence intensity was also introduced to evaluate the relative proliferation of the HUVECs and HUASMCs in the coculture model, and the SMCs-ColIV-ECs showed more HUVECs and less SMCs as compared with the SMCs-HAa-ECs relatively. The retention of HUVECs in the SMCs-ColIV-ECs model was also significantly enhanced compared with SMCs-HAa-ECs and the HUVECs alone groups. The patterned coculture models were anticipated to provide helpful and practical application for building and studying the human vascular bionic endometrial *in vitro*.

REFERENCES

1. Wang HQ, Bai L, Shen BR, Yan ZQ, Jiang ZL. Coculture with endothelial cells enhances vascular smooth muscle cell adhesion and spreading via activation of β1-integrin and phosphatidylinositol 3-kinase/Akt. Eur J Cell Biol 2007;86:51–62.
2. Mark DL, Zheng P, Charles SW, Laura EN, George AT. A system for the direct co-culture of endothelium on smooth muscle cells. Biomaterials 2005;26:4642–4653.
3. Chiua JJ, Chen LJ, Chen CN, Lee PL, Lee CI. A model for studying the effect of shear stress on interactions between vascular endothelial cells and smooth muscle cells. J Biomech 2004;37:531–539.
4. Cao L, Wu A, Truskey AG. Biomechanical effects of flow and coculture on human aortic and cord blood-derived endothelial cells. J Biomech 2011;44:2150–2157.
5. Agelikie GV, Lin LF, Marc DB. Pressure and endothelial coculture upregulate myocytic Fas–FasL pathway and induce apoptosis by way of direct and paracrine mechanisms. Am J Surg 2005;190:780–786.
6. Fillinger MF, Sampson LN, Cronenwett JL, Powell RJ, Wagner RJ. Coculture of endothelial cells and smooth muscle cells in bilayer and conditioned media models. J Surg Res 1997;67:169–178.
7. Marc H, David M, Frédéric P, Peter D, Serge A, Saadia E. Endothelial cell dysfunction and cross talk between endothelium and smooth muscle cells in pulmonary arterial hypertension. Vasc Pharmacol 2008;49:113–118.
8. Tull SP, Anderson SI, Hughan SC. Cellular pathology of atherosclerosis—Smooth muscle cells promote adhesion of platelets to cocultured endothelial cells. Circ Res 2006;98:98–104.
9. Li JA, Li GC, Zhang K, Liao YZ, Yang P, Maitz FM, Huang N. Coculture of vascular endothelial cells and smooth muscle cells by hyaluronic acid micro-pattern on titanium surface. Appl Surf Sci 2013;273:24–31.
10. Price RD, Berry MG, Harshad AN. Hyaluronic acid: The scientific and clinical evidence. J Plast Reconstr Aesthet Surg 2007;60:1110–1119.
11. Li GC, Yang P, Qin W, Maitz MF, Zhou S, Huang N. The effect of coimmobilizing heparin and fibronectin on titanium on hemocompatibility and endothelialization. Biomaterials 2011;32:4691–4703.
12. Li JA, Yang P, Zhang K, Ren HL, Huang N. Preparation of SiO_2/-TiO_2 and TiO_2/TiO_2 micropattern and their effects on platelet adhesion and endothelial cell regulation. Nucl Instrum Methods B 2013;307:575–579.
13. Luo RF, Tang LL, Wang J, Zhao YC, Tu QF, Weng YJ, Shen R, Huang N. Improved immobilization of biomolecules to quinone-rich polydopamine for efficient surface functionalization. Colloid Surf B 2013;106:66–73.
14. Lei LJ, Li CH, Yang P, Huang N. Photo-immobilized heparin micropatterns on Ti–O surface: Preparation, characterization, and evaluation in vitro. J Mater Sci 2011;46:6772–6782.
15. Chen JL, Li QL, Chen JY, Chen C, Huang N. Improving blood-compatibility of titanium by coating collagen–heparin multilayers. Appl Surf Sci 2009;255:6894–6900.

16. Li GC, Zhang FM, Liao YZ, Yang P, Huang N. Coimmobilization of heparin/fibronectin mixture on titanium surfaces and their blood compatibility. Colloid Surf B 2010;81:255–262.
17. Tu QF, Zhang Y, Ge DX, Wu J, Chen HQ. Novel tissue-engineered vascular patches based on decellularized canine aortas and their recellularization in vitro. Appl Surf Sci 2008;255:282–285.
18. Kielty CM, Whittaker SP, Grant ME, Shuttleworth CA. Type IV collagen microfibrils: evidence for a structural association with hyaluronan. J Cell Biol 1992;118:979–990.
19. Wang BC, Tang CH, Zhu LC, Chen Q. Investigation on the effects of diamide on NO production in vascular endothelial cells (VEC). Colloid Surf B 2004;35:205–208.
20. Jestis MM, Angeles RM. Role of vascular nitric oxide in physiological and pathological conditions. Pharmacol Ther 1997;75:111–134.
21. Welch G, Loscalzo J. Nitric oxide and the cardiovascular system. J Cardiovasc Surg 1994;9:361–371.
22. Minamiyama Y, Takemura S, Inoue M. Albumin is an important vascular tonus regulator as a reservoir of nitric oxide. Biochem Biophys Res Commun 1996;225:112–115.
23. Keri BV, Sean JK, Stephen RH, Monica TH. Endothelial cell cytoskeletal alignment independent of fluid shear stress on micropatterned surfaces. Biochem Biophys Res Commun 2008;371: 787–792.
24. Boswell MG, Zhou W, Newcomb DC, Peebles RS Jr. PGI_2 as a regulator of CD4+ subset differentiation and function. Prostaglandins Other Lipid Mediat 2011;96:21–26.
25. Whittaker N, Bunting S, Salmon J, Moncada S, Vane JR, Johnson RA, Morton DR, Kinner JH, Gorman RR, McGuire JC, Sun FF. The chemical structure of prostaglandin X (prostacyclin). Prostaglandins 1976;12:915–928.
26. Helliwell RJ, Adams LF, Mitchell MD. Prostaglandin synthases: Recent developments and a novel hypothesis. Prostaglandins Leukot Essent Fatty Acids 2004;70:101–13.
27. Tu QF, Zhao YC, Xue XQ, Wang J, Huang N. Improved endothelialization of titanium vascular implants by extracellular matrix secreted from endothelial cells. Tissue Eng Part A 2010;16: 3635–3645.